

# Discovery of extended radio emission in the young cluster Wd1

J.S. Clark<sup>1,2</sup>, R.P. Fender<sup>1,3</sup>, L.B.F.M. Waters<sup>3</sup>, S.M. Dougherty<sup>4</sup>, J. Koornneef<sup>5</sup>,  
I. A. Steele<sup>6</sup>, and A. van Blokland<sup>3</sup>

<sup>1</sup> *Astronomy Centre, University of Sussex, Falmer, Brighton, BN1 9QH, UK*

<sup>2</sup> *Department of Physics and Astronomy, University of Southampton, Southampton, SO17 1BJ, UK*

<sup>3</sup> *Astronomical Institute Anton Pannekoek, University of Amsterdam and Center for High Energy Astrophysics, Kruislaan 403, 1098 SJ Amsterdam, Netherlands*

<sup>4</sup> *University of Calgary/DRAO, PO Box 248, White Lake Rd, Penticon, B.C., V2A 6K3 Canada*

<sup>5</sup> *Kapteyn Astronomical Institute, University of Groningen, Groningen, 9700 AV, The Netherlands*

<sup>6</sup> *Astrophysics Group, Liverpool John Moores University, Liverpool, L3 3AF, UK*

Version 21 May 1998

## ABSTRACT

We present 10  $\mu\text{m}$ , ISO-SWS and Australia Telescope Compact Array observations of the region in the cluster Wd1 in Ara centred on the B[e] star Ara C. An ISO-SWS spectrum reveals emission from highly ionised species in the vicinity of the star, suggesting a secondary source of excitation in the region. We find strong radio emission at both 3.5cm and 6.3cm, with a total spatial extent of over 20 arcsec. The emission is found to be concentrated in two discrete structures, separated by  $\sim 14''$ . The westerly source is resolved, with a spectral index indicative of thermal emission. The easterly source is clearly extended and nonthermal (synchrotron) in nature. Positionally, the B[e] star is found to coincide with the more compact radio source, while the southerly lobe of the extended source is coincident with Ara A, an M2 I star. Observation of the region at 10  $\mu\text{m}$  reveals strong emission with an almost identical spatial distribution to the radio emission. Ara C is found to have an extreme radio luminosity in comparison to prior radio observations of hot stars such as O and B supergiants and Wolf-Rayet stars, given the estimated distance to the cluster. An origin in a detached shell of material around the central star is therefore suggested; however given the spatial extent of the emission, such a shell must be relatively young ( $\tau \sim 10^3$  yrs). The extended non thermal emission associated with the M star Ara A is unexpected; to the best of our knowledge this is a unique phenomenon. SAX (2–10keV) observations show no evidence of X-ray emission, which might be expected if a compact companion were present.

**Key words:** stars:individual(Ara C) - stars:emission line, B[e] - stars:radio emission

## 1 INTRODUCTION

B[e] stars are characterised by a large infrared excess, thought to be due to hot dust at  $\sim 10^3$  K. In this respect the B[e] stars differ from classical Be stars, where the IR excess is due to free free emission from hot gas. Spectroscopically B[e] stars differ from classical Be stars due to the presence of narrow forbidden line emission from singly ionised metals, such as  $\text{Fe}^+$  in addition to strong Balmer line emission at optical wavelengths. UV spectra reveal species with a much higher degree of ionisation than seen in optical spectra, in an analogous manner to classical Be stars. This fact led Zickgraf

et al. (1986) to propose a two component wind to explain the spectra, with a slowly expanding cool equatorial component responsible for the optical spectral features, and a hotter, high velocity polar component producing the high excitation features in the UV spectra. Near IR observations of B[e] stars by McGregor et al. (1988) and subsequently Morris et al. (1996) reveal Na I and CO bandhead emission, confirming the presence of cooler circumstellar regions as indicated by the dust emission.

The spectra also show a similarity between B[e] stars and both Be supergiant and LBV spectra. On the basis of

the morphological similarities between the spectra they suggest a close evolutionary link between the three types of star. If confirmed this would be an important result, as there is still some confusion as to the exact evolutionary status of B[e] stars (see for example Lamers et al. 1998). In order to investigate the evolutionary status of these objects, observations of the galactic B[e] star Ara C were made as it is the only known galactic B[e] star in a cluster, permitting an accurate measurement of its luminosity, and hence age (since very very luminous young B[e] stars are not expected to be seen).

## 2 THE ARA CLUSTER

The diffuse object in Ara found at  $2.2\mu\text{m}$  by Price (1968) was identified by Westerlund (1968) as a heavily reddened cluster. Further work by Borgman et al. (1970), Koornneef (1977) and most recently Westerlund (1987) have done much to clarify the properties of the cluster. The cluster is thought to be young, with an age of only  $\sim 7$  million years (Westerlund 1987). The distance is estimated to be  $\sim 5.2\text{kpc}$ , which gives a cluster size of some  $3\text{pc}$ , within which photometry is available for some  $\sim 258$  stars (Westerlund 1987). The cluster is heavily reddened, with  $A_V \sim 11$ , of which  $A_V = 7$  is thought to be due to dust in the region of the cluster. Westerlund (1987) estimates a minimum mass of  $\sim 20M_\odot$ , which implies the presence of  $\sim 2000M_\odot$  of gas compared to  $1200M_\odot$  to be found in 82 of the brightest cluster stars (lower limiting luminosity of  $\log L/L_\odot = 3.5$ ). The diffuse  $H\alpha$  emission seen in images of the cluster is attributed to excitation by the stellar radiation fields.

The intrinsically brightest stars of the cluster form a continuous sequence from B2 Ia to M2 Ia. Below the supergiant sequence Westerlund (1987) finds that most of the stars are luminosity class II-III, with the faintest stars on the main sequence. Ara C, identified as star 9 in Westerlund (1987), was of immediate interest due to a remarkable emission line spectrum, consisting of very strong Balmer emission ( $EW_{H\alpha} \sim 250\text{\AA}$ ), HeI emission, as well as FeII, [NII], [OII] and [ArIII]. Westerlund classified the star as Be, but the  $H\alpha$  equivalent width is at least a factor 5 higher than the largest values reported for classical Be stars, and comparison with the spectra of other massive emission line objects suggests that star C may be a B[e] star. Due to uncertainty in the intrinsic colours of B[e] stars, the values of  $M_v \sim 6$  and  $A_v \sim 8.70$  derived for Ara C in Westerlund (1987) are the subject of some uncertainty. Likewise, the estimate of  $\log(L_*/L_\odot) = 4.86$  for Ara C was derived under the assumption of  $T_{eff} \sim 20000\text{K}$ , and should be treated with caution.

Many B[e] stars are known in our Galaxy, but their nature is unclear, since their spectral characteristics coincide closely with those of massive YSO's. The situation would improve if B[e] stars could be identified in clusters, as is proposed for Ara C. This implies that Ara C is a post-main-sequence object since the age of the cluster is such that massive stars can no longer be YSO's. This is, to the best of our knowledge, the first case in which a galactic B[e] star can definitively be classified as a post-main-sequence object, which demonstrates that Galactic counterparts to the LMC B[e] supergiants, as discussed by Zickgraf et al. (1986), do exist.

## 3 OBSERVATIONS

### 3.1 ISOCAM, ISO-SWS and TIMMI observations

ISOCAM images at  $\sim 3\text{-}10\mu\text{m}$  of the Ara C region were made on 1996 September 10. The ISOCAM data were taken with the 1.5 pixel field of view (FOV) setting. The array is  $32 \times 32$  pixels and so the total FOV is about  $47 \times 47$  arcsec (the PSF for the wavelengths used can be calculated from Cesarsky et al 1996). The  $3\mu\text{m}$  image shows Ara C to be an unresolved point source (several other bright stars in the cluster are also visible as point sources). Ara C is also visible in the  $10\mu\text{m}$  image as a point source, as is Ara A (nomenclature by Borgman et al 1970; denoted star 26 by Westerlund 1987).

Based on a combination of low resolution optical spectroscopy and photometry Westerlund (1987) classifies this as an M2 I star, with a bolometric luminosity of  $\log(L_*/L_\odot) = 5.26$  and an effective temperature of  $\log(T_{eff}) = 3.54$ . Further extended emission is visible to the north of this source in the  $10\mu\text{m}$  image. A  $10\mu\text{m}$  TIMMI image is shown in Figure 2, and confirms the the identification of extended emission to the north of Ara A (TIMMI is fully described in Käufel et al 1992; the broad band N filter was used in the observations). Due to its absence from the  $3\mu\text{m}$  image this is most likely due to emission from cold dust (compared to the warmer dust thought to be responsible for the unresolved emission centred on Ara C and Ara A).

A fast SWS spectrum centred on Ara C was also obtained at this time (ISO-SWS is fully described in De Graauw et al. 1996). The spectral range employed was  $2.4\text{-}45\mu\text{m}$ ; gaussian fits to the strongest forbidden lines are presented in Figure 3. This was expected to yield information on the presence and composition of circumstellar dust, and forbidden line emission (we note that based on the presence of both emission lines in the spectrum, and hot dust associated with the star, the classification of Ara C as a B[e] star is confirmed). There is no evidence in the spectrum for the presence of the Unidentified Infrared (UIR) emission bands  $3.29$ ,  $6.2$ ,  $7.6/7.7$ ,  $8.6$ ,  $11.3$ , and  $12.7\mu\text{m}$  that tend to occur together. These features are referred to by Tokunaga (1996) as 'carbonaceous emission bands', and are sometimes attributed to polycyclic aromatic hydrocarbons (PAHs), which might be expected to arise in the dusty circumstellar envelope. However, a strong narrow emission feature is visible at  $20.59\mu\text{m}$ , possibly due to a simple oxide (although an association with crystalline silicates cannot be ruled out at this time). The spectrum also revealed the presence of [O IV]. These observations are deeply puzzling, as this observation implies temperatures of  $\sim 80,000\text{K}$ , which cannot be due to the stellar radiation field ( $\sim 20,000\text{K}$ ), and clearly imply the presence of another source of ionising radiation in the system. It should be noted that there is likely to be some contamination from the M2 I star Ara A in the spectrum, and so the exact location of the highly ionised gas cannot be conclusively identified with the circumstellar environment of Ara C from this observation alone.

### 3.2 Radio Observations

In a survey of bright Southern radio sources Wright et al. (1994) report a detection of a point source at co-ordinates RA 16 47 07.5, Dec -45 50 39.0 (J2000; designated PMNJ

1647-4550 in their catalogue),  $\sim 20''$  of RA from the optical co-ordinates reported for Ara A. They estimate an error of  $6.9''$  in RA, making the position of the point source  $\sim 3\sigma$  from the extended near-IR source reported here. However, no other radio source within 5 arcmin is reported by the SIMBAD database, and so we conclude that despite the discrepancy in the positions, PMNJ 1647-4550 is likely to correspond to the resolved emission associated with Ara A and C.

Observations of the Ara C region at 3.6 and 6.3cm were obtained with the Australian Telescope Compact Array (ATCA) on 1997 April 30. These observations were interleaved with those of a nearby phase referenced source (1646-50), with a total on source integration of 93 minutes. The flux scale was determined by observations of J1934-638. After determining initial antennae gain solutions by phase referencing, the gain solutions were improved by three iterations of self-calibration.

Strong radio emission at both 3.5 and 6.3 cm was detected at the expected position of Ara C, and in an extended structure  $\sim 10$  arcsec to the east (Figure 1). The eastern emission is concentrated into two lobes which we label Ara A (North) and Ara A (South) respectively. We find that the emission associated with Ara C is thermal in nature (positive spectral index) while that of Ara A(N & S) is nonthermal in origin (negative spectral index). Examination of the radio images suggests that Ara C can be closely represented by a 2D gaussian. To estimate the size of Ara C we have examined the visibility data directly. After locating the peak of Ara C at the phase-tracking centre of the image, we removed the flux contributed from Ara A(S) and Ara A(N) using the AIPS routine UVSUB. The remaining visibilities were then binned into a  $15 \times 15$  grid to improve the signal-to-noise ratio. These visibilities clearly show that Ara C is resolved by the array. A two-dimensional Gaussian fit to this gridded data then gives an estimate of the source size, the total flux of the source and the position angle of the emission distribution (see Tables 1 and 2). For comparison, we also estimated the source size by fitting two-dimensional-Gaussian functions to the image of Ara C (AIPS routine JMFIT). These give the same results as the visibility fitting within the uncertainties.

The coordinates of the Gaussian fit to the western compact radio condensation are RA 16 47 04.2 Dec -45 50 31.6 (J2000). An estimate for the position of Ara C of RA 16 47 04.2 Dec -45 50 30.7 was derived from a combination of the ISO-CAM image and an STScI DSS image (ie within 1 arcsec of the radio co-ordinates). In Figure 2 we overplot the  $10\mu\text{m}$  TIMMI image on the 6.3cm map, centering both image and map on Ara C (ISOCAM fluxes for Ara C and Ara A of  $\sim 50\text{Jy}$  and  $\sim 190\text{Jy}$  respectively). We find an excellent coincidence between emission at both wavelengths in both lobes of Ara A. Optical co-ords for Ara A(S) are RA 16 47 05.25 Dec -45 50 39. Radio co-ords for Ara A(S) and Ara A(N) are RA 16 47 05.42 Dec -45 50 36.7 and RA 16 47 05.85 Dec -45 50 29.66 respectively. We further plot the positions of other cluster stars on this image (notation by Borgman et al 1970). We cite the excellent agreement of these positions with the TIMMI image as evidence for the identification of Ara C with the westerly radio source. We further note that our co-ordinates are consistent, within the quoted errors, to all prior published positions.

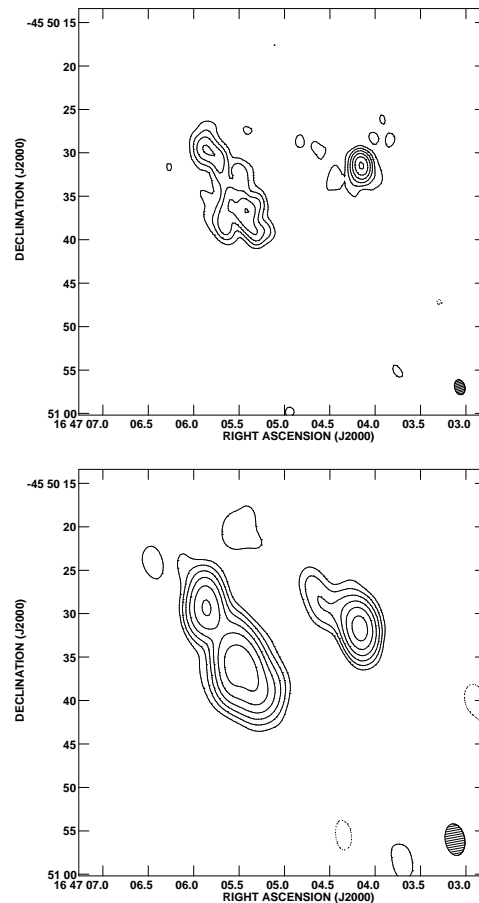


**Figure 1.** 3.5 cm (upper) and 6.3 cm (lower) maps of the region surrounding Ara A and Ara C (contours are at -1, 1, 2, 4, 8, 16, 32, 64, 128 and 256 times the r.m.s. noise level of 1.1mJy and 1.5mJy respectively). Beam sizes are indicated in the lower right corner of each panel ( $1.8 \times 1.2$  arcsecs at 14 degrees and  $3.7 \times 2.3$  arcsecs at 10 degrees for 3.5cm and 6.3cm respectively).

|           | Integrated flux |                 | Spectral Index   |
|-----------|-----------------|-----------------|------------------|
|           | 3.5cm (mJy)     | 6.3cm (mJy)     |                  |
| Ara C     | $51.7 \pm 0.6$  | $41.8 \pm 0.5$  | $0.36 \pm 0.03$  |
| Ara A (S) | $92.4 \pm 1.0$  | $125.4 \pm 0.8$ | $-0.52 \pm 0.02$ |
| Ara A (N) | $30.1 \pm 0.7$  | $35.8 \pm 0.4$  | $-0.30 \pm 0.04$ |

**Table 1.** Flux data for the source coincident with Ara C and the 2 components of the emission coincident with Ara A.

| Wavelength | Source Size (milli arcsec)      | Position Angle    |
|------------|---------------------------------|-------------------|
| 3.5cm      | $954 \pm 24 \times 523 \pm 18$  | $166^\circ \pm 3$ |
| 6.3cm      | $1179 \pm 74 \times 732 \pm 51$ | $10^\circ \pm 5$  |

**Table 2.** Source size for Ara C (derived from visibility fitting)

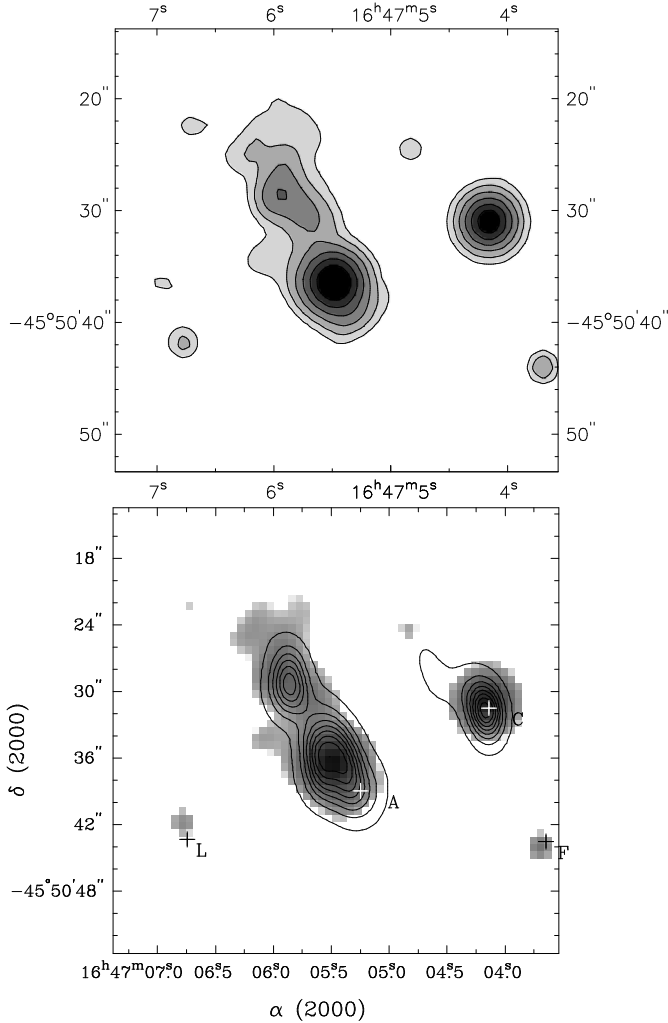


**Figure 2.** Upper Panel: TIMMI  $10\mu\text{m}$  image of the field (fluxes derived from ISOCAM observations of  $\sim 50\text{Jy}$  and  $\sim 190\text{Jy}$  for Ara C and Ara A respectively). Lower Panel: overlay of the TIMMI (greyscale) and  $6.3\text{cm}$  (contour) plots. The positions of other cluster stars (notation by Borgman et al 1970) are also shown.

#### 4 DISCUSSION

The spectral index of the source Ara C is suggestive of thermal emission, possibly from a stellar wind. However the spectral index ( $\alpha=0.36\pm 0.03$ ) clearly departs from that expected for either an isothermal, spherically symmetric wind of constant velocity ( $\sim 0.6$ ) or an optically thick wind ( $\alpha=2.0$ ). Given the distance estimates of  $\sim 5.2\text{kpc}$ , the implied radio luminosity is in excess of any previously observed OB supergiant or Wolf Rayet, comparable only to certain Luminous Blue Variables (LBVs). If the radio luminosity is attributed solely to a stellar wind, this implies an excessive mass loss rate given the bolometric luminosity of the star. Likewise, the fact that the emission is extended argues against attributing the flux to a stellar wind; the emitting region is two orders of magnitude larger than the effective radii for free-free radio emission from OB stars reported by Lamers & Leitherer (1993), for example. Consequently, we propose that the radio flux is produced by a two component

**Figure 3.** Line profiles for the strongest forbidden lines in the ISO-SWS spectrum. Data points from the up and down scans are shown separately. The nominal (solid line) and best fit (broken line) wavelengths are also indicated.

model consisting of a (partially) optically thick stellar wind, and an extended optically thin component produced by reradiation. This could be the result of emission from ambient intracluster material (although the previous main sequence wind regime might have cleared a cavity around the star), or from a detached shell of material surrounding the star. A similar structure has been observed before in radio and IRAS observations of G79.29+0.46, with an optically thin detached shell of material centred on a stellar source with a partially optically thick radio spectrum (Higgs et al. 1994, Waters et al. 1996). Waters et al. (1996) conclude that the present day wind characteristics of this star suggest that it could be a member of the class of Luminous Blue Variables (LBVs), while the detached shell is either the result of a Red Supergiant (RSG) phase, or an extended period of LBV-like mass loss.

Could Ara C also be an LBV? Based on morphological similarities between K-band spectra of B[e] and LBVs Morris et al. (1996) have suggested a close connection between the two types of star. With a bolometric luminosity of  $\log(L_*/L_\odot)=4.86$ , Ara C lies below the observed range of luminosities for LBV's ( $\log(L_*/L_\odot)\geq 5-6$ ) reported by Hutsemékers & van Drom (1991); however a lower luminosity limit to LBV behaviour is not known with certainty at present. Such a luminosity suggests that Ara C has only recently started to evolve off the main sequence of the HR diagram towards the RSG region, and so doubts must exist as to whether it could have produced a detached shell of material in such a short period of time. We note that an error of  $\sim 20$  per cent in the distance estimates to the cluster, an

underestimate of  $A_v$  (possibly due to local inhomogeneities in the intra cluster medium) or uncertainties in the spectral type of the star (and hence bolometric correction) could result in an increase in the bolometric luminosity of Ara C to  $\log(L_*/L_\odot)=5.0$ . Such a luminosity would then place it in the region of the HR diagram occupied by LBVs (and would also allow it to have evolved through a RSG phase). Unfortunately due to lack of high resolution spectral or radio observations it is not possible to extract information on the present wind characteristics of Ara C, and so it is not possible to determine a present day mass loss rate or terminal wind velocity, both of which would help to determine the evolutionary status of the star. However, it is possible to estimate the age of the detached shell from its angular extent (given in Table 2). If the distance to the cluster is taken to be 5.2kpc, and a value of  $30\text{kms}^{-1}$  is adopted for the terminal wind velocity (appropriate for a RSG; Waters et al 1996), then the age of the shell is found to be  $\sim 600\text{yrs}$ . Since Maeder & Meynet (1988) estimate the time taken for massive stars to evolve from the red to blue region of the HR diagram to be  $1-3 \cdot 10^4\text{yr}$ , this would tend to argue against the shell being formed during a RSG phase (although it should be noted that the higher densities of the ISM expected in this cluster could affect the shell expansion velocity).

An explanation for the nonthermal emission positionally coincident with Ara A is more problematic. Previous observations of M-type giants and supergiants (for example Reid & Menton 1996, Skinner et al. 1996) have revealed them to be radio sources. The emission has been attributed to free-free emission in a radio photosphere extending a few AU. However, the nonthermal nature of the emission observed clearly eliminates this possibility. Radio emission from OH masers has also been observed in some systems, with individual masers lying at up to  $\sim 500\text{AU}$  from the star. However, at an estimated distance of  $\sim 5.2\text{kpc}$ , the extended emission along the NE/SW axis is  $\sim 10^5\text{AU}$  long,  $\sim 10^3$  times larger than the distance at which OH masers are seen. The low resolution optical spectrum of Westerlund (1987) shows low level H  $\alpha$  emission, which possibly originates from excited gas associated with the dust seen in the TIMMI image. No other lines are seen in emission in this spectrum, ruling out the identification of the M2 I star as a component in a symbiotic system, since symbiotic systems typically show a wealth of emission lines in their spectra. Given the linear structure of the emission, it is tempting to attribute it to jet emission from accretion onto a compact object. Such a scenario appears to be excluded by SAX 2-10keV observations, which provide an upper limit of 10 milliCrab to any emission (ie a lower luminosity than expected for a neutron star accreting at the Eddington limit; J. Heise priv. comm.), but we note that possible X-ray emission might be softer than that detectable by SAX, or such a source might be a transient source of X-rays. Likewise, given the current observations we are unable to excluded the possibility of a chance alignment between Ara A and a background radio source.

## 5 CONCLUSIONS

Motivated by ISO SWS observations of the source Ara C we have obtained radio observations at 6.3cm and 3.5cm. These observations resulted in two strong detections, one compact

source coincident with the optical coordinates of Ara C, and a second extended source, the southernmost lobe of which is coincident with Ara A, an M2 I star. An analysis of the spectral indexes of these two detections reveals that the emission associated with Ara C is most likely thermal in origin, while that associated with Ara A is non thermal. Comparison to  $10 \mu\text{m}$  images of the region shows a remarkable coincidence between radio and IR continuum emission (thought to arise from hot dust).

The physical processes giving rise to the emission are not clear. Despite the thermal nature of the emission associated with Ara C, it would appear unlikely that the emission is the result of a steady stellar wind, with both luminosity and its resolved nature arguing against such an interpretation. A more plausible scenario would appear to be emission from a combination of a compact, partially optically thick stellar wind, and an extended optically thin source, possibly a detected shell of material formed in a possible RSG or LBV phase. The relationship between the eastern emission component and Ara A and C is as yet unclear. Despite the positional coincidence between the southernmost lobe of both radio and  $10\mu\text{m}$  emission and Ara A it is uncertain whether the emission is associated with this star or the result of a chance alignment. We note that if emission is associated with Ara A then it would be the first observation of non thermal radio emission from an M supergiant.

## REFERENCES

- Borgman J., Koornneef J., Slingerland J., 1970, A&A, 4, 248.  
 Cesarsky C. J., Abergel A., Agnese B., et al., 1996, A&A, 315, L32.  
 De Graauw Th., Haser L.N., Beintema D.A., et al., 1996, A&A 315, L49-L54.  
 Higgs L.A., Wendker H.J., Landecker T.I., 1994, A&A, 291, 295.  
 Hutsemekers D., van Drom E., 1991, A&A, 251, 620.  
 Käufel, U., Jouan, R., Lagage, P. O., Masse, P., Mestreau, P., Tarrrius, A.: 1992, The Messenger 70, 67  
 Koornneef J., 1997, A&A, 55, 469.  
 Lamers H. J. G. L. M., Leitherer C., 1993, ApJ 412, 771.  
 Leitherer C., Chapman J. M., Koribalski B., 1995, ApJ, 450, 289.  
 Maeder A., Meynet G., 1988, A&ASS, 76, 411.  
 Marlborough J. M., Dougherty S. M., 1991, A&A 244, 120.  
 McGregor P. J., Hyland A. R., Hillier D. J., 1988, ApJ, 324, 1071.  
 Morris P. W., Eenens P. R. J., Hanson M. M., Conti P. S., Blum R. D., 1996, ApJ, 470, 597.  
 Reid M. J., Menton K. M., in Radio Emission from the Stars and the Sun, ASP Conf. Series, Vol 93, 1996, A. R. Taylor and J. M. Paredes (eds), 1996, 87.  
 Skinner C. J., Dougherty S. M., Bode M. F., Drake S., Davis R. J., 1997, MNRAS, 288,295.  
 Tokungaa A. T., 1996, Paper presented at 'Diffuse Infrared Radiation and the IRTS', Tokyo, November 1996 (preprint IFA-97/13: 'A Summary of the 'UIR' Bands'.  
 Waters L.B.F.M., Izumiura H., Zaal P.A., Geballe T.R., Kester D.J.M., Bontekoe Tj.R., 1996, A&A, 313, 866.  
 Westerlund B., E., 1968, ApJ, 154, L67.  
 Westerlund B. E., 1987, A&ASS, 70, 311.  
 Wright A. E., Griffith M. R., Burke B. F., Ehers R. D., 1994, ApJSS, 91, 111.  
 Zickgraf F.-J., Humphreys R. M., Lamers H. J. G. L. M., Smolinski J., Wolf B., Stahl O., 1996, A&A, 315, 510.

